Title
EFFECT OF MICROSTRUCTURE ON DEFORMATION OF POLYCRYSTAL-LINE MAGNESIUM OXIDE

Authors
Langdon, Terence G.
Pask, Joseph A.

Publication Date
1970-11-01

Submitted to Journal of the
American Ceramic Society

UCRL-17831
Preprint

EFFECT OF MICROSTRUCTURE ON DEFORMATION OF POLYCRYSTALLINE MAGNESIUM OXIDE

Terence G. Langdon and Joseph A. Pask

November 1970

AEC Contract No. W-7405-eng-48

LAWRENCE RADIATION LABORATORY
UNIVERSITY of CALIFORNIA BERKELEY

DISCLAIMER

EFFECT OF MICROSTRUCTURE ON DEFORMATION OF POLYCRYSTALLINE MAGNESIUM OXIDE**

Terence G. Langdon* and Joseph A. Pask

Inorganic Materials Research Division, Lawrence Radiation Laboratory
and Department of Materials Science and Engineering,
College of Engineering, University of California,
Berkeley, California

ABSTRACT

October 1970

Six different types of polycrystalline magnesium oxide, one nominally fully-dense and the others having porosities of ∿1-2%, were tested in compression at temperatures up to 1400°C. At temperatures of 1200°C and above, all materials deformed plastically; but two of the materials, both porous, also exhibited plastic flow at temperatures down to 800°C, and a third at 1000°C. A qualitative analysis of the microstructures of these materials indicated that the differences in behavior primarily arose because of variations in the size and distribution of pores and in the concentration of impurities at the grain boundaries. It is suggested that the following factors aid plasticity at temperatures below ∿1200°C: (i) strong grain boundaries in the absence of excessive impurities, permitting the build-up of stress concentrations with the consequent nucleation of slip on the {100} system and the extension of slip across the boundaries, and (ii) clusters of very fine pores within the grains, which allow some mass accommodation.

---

* Now at Department of Metallurgy, University of British Columbia, Vancouver 8, B.C., Canada.

** Presented in part at the Twentieth Annual Pacific Coast Regional Meeting, American Ceramic Society, San Francisco, California, November 3, 1967 (Basic Science II).

I. INTRODUCTION

Much attention has been devoted to an evaluation of the mechanical behavior of magnesium oxide single crystals under various experimental conditions; but only limited work has been carried out on polycrystalline MgO because of the difficulties of obtaining specimens with controlled microstructures (characters) and of characterizing porous, and thus two-phase, systems. The few investigations reported with polycrystals have invariably dealt with material in which the porosity was not evaluated in terms of average pore size or distribution (i.e. whether the pores were located primarily along the grain boundaries or within the matrix).

Experiments by Copley and Pask[1] indicated that the size and distribution of pores may markedly affect the mechanical behavior, since a material having very small pores both within the grains and along the boundaries was ductile at temperatures as low as 800°C, whereas four other materials, including one which was nominally fully-dense, were all brittle up to temperatures of ∿1200°C. This suggested that ductility may be realized in a slightly porous material because the few pores present were sufficient to initiate slip, but the desirable relationships between grain size, pore size and/or pore location were not investigated.

Tests on metals having porosities of 10-30% have demonstrated that mechanical behavior is often influenced by character features other than the total volume of porosity <u>per se</u>;[2] but no definitive tests have apparently been carried out to study the importance of pore distribution for the much lower total porosities usually associated with polycrystalline ceramics. The present investigation was therefore undertaken to evaluate the significance of porosity in polycrystalline MgO under controlled

experimental conditions.

II. EXPERIMENTAL PROCEDURE

(1) Material

Tests were carried out on five different types of polycrystalline MgO (Types 1-5), covering a range of grain size and porosity. A spectrographic analysis of each type is given in Table I. To permit a direct comparison with the earlier work of Copley and Pask,[1] their "Type 2" material, which showed ductility at temperatures as low as 800°C, is also included in Table I as Type 6. Typical microstructures of each material are shown in Fig. 1, and the primary characteristics are listed in Table II. A more detailed description follows:

Type 1. Transparent polycrystalline MgO was produced in this laboratory by hot-pressing MgO powder with an LiF additive, using the technique developed by Rice[3] and described in detail elsewhere.[4]

High purity MgO powder (Baker and Adamson reagent grade) was mixed with 3 wt% LiF (Baker reagent grade) in isopropyl alcohol, dried in an oven, and then hot-pressed in vacuum in a graphite die. A constant pressure of 1200 psi was applied at room temperature, and maintained constant while the temperature was raised to 1000°C over a period of ∿3 h. Specimens were held at temperature for 3 h, and then furnace-cooled to give translucent disks approximately 1.5 in. in diameter and 0.25 in. thick. The average grain size in this condition was ∿2-3 μm, and the second column of Table I, Type 1(a), refers to the material at this stage of the fabrication process. Following hot-pressing, all specimens were annealed for 3 h at 1300°C, to give transparent disks with an average grain size of ∿12 μm.

As shown in Table I, the small amount of lithium remaining after hot-pressing was predominantly removed by the subsequent heat-treatment at 1300°C, although 75 ppm was still present in the final material. Using transmission electron microscopy, it was established that there was no second phase in this material, even at the grain boundaries or triple points;[5] but differences in fracture behavior between Type 1 and the other materials suggest that the residual LiF was probably preferentially segregated along the boundaries in solid solution.

Type 2. Specimens of Types 2-6 were obtained commercially* in the form of white, slightly translucent, tiles of approximate dimensions 1.25 in. x 1.25 in. x 0.25 in. These were produced by isostatic pressing and sintering, with the manufacturing conditions varied in each case to give different degrees of porosity and pore distribution; further details of the fabrication procedure are given elsewhere.[6]

Specimens of Type 2 had many large pores on the grain boundaries and at triple points; in some instances, elongated pores, up to ∿10 μm in length, spread along the boundaries. In addition, the average size of the pores on the boundaries (∿4 μm) was large relative to the average grain size (ratio of 0.20). Smaller pores existed within the grains, with some evidence of clustering.

Type 3. The pores on the grain boundaries (∿2.0 μm) were small with respect to the average grain size (ratio of 0.05). Within the grains, the pores were usually very small and in clusters. The whitish blotches visible in the microstructure in Fig. 1, and also to a lesser extent in

*Honeywell, Inc., Minneapolis, Minnesota.

Types 4-6, may be associated with the higher SiO_2 and CaO contents of these materials.

Type 4. The pore distribution was fairly uniform, with less evidence of clustering. As a result, only a small number of pores existed on the boundaries; these were invariably small relative to the average grain size (ratio of 0.02).

Type 5. This material was similar to Type 6, but with a larger grain size due to an anneal at 1800°C. Large pores, up to ∿5 μm in diameter, were located on the boundaries, but these were small with respect to the grain size (ratio of 0.05). Clusters of extremely small pores existed predominantly in the centers of the larger grains.

Type 6. Extremely fine pores existed in large clusters within the grains. On the boundaries, the pores were small relative to the average grain size (ratio of 0.04).

A comparison of the microstructures of Types 5 and 6 suggests that the pore-free regions adjacent to the grain boundaries in Type 5 represent the areas swept out by the moving boundaries during the grain growth at 1800°C. The existence of these large regions at grain edges, and the fact that the average size of pores on the boundaries is larger in Type 5 than Type 6, indicates that the pores migrate with the boundaries during grain growth. This is substantiated by noting that the average pore size is approximately linearly proportional to the grain size.[7]

(2) Preparation and Examination of Specimens

Test specimens were cut from the disks and tiles with a diamond saw to approximate dimensions 1.0 in. x 0.25 in. x 0.25 in., and the ends ground perpendicular to the longitudinal axis using a special jig. To

permit detailed examination before and after deformation, one face of each specimen was polished on successively finer grades of abrasive paper, and then lapped with 1-2 μm diamond paste followed by 0.3 μm alumina slurry on a high-speed wheel. After masking the ends in a lacquer ("Stoner-Mudge"), the specimens were chemically polished by immersing for 1 min. in 85% H_3PO_4 heated to 150-155°C, and then washed in boiling distilled water, methyl alcohol, and ether. All four faces were polished since it is known that, for both single and polycrystals, the deformation characteristics are affected by the presence of submicroscopic surface damage.[6,8-10] The lacquer was removed prior to testing using methyl-ethyl-ketone.

Undeformed specimens were etched in a solution of two parts 85% H_3PO_4 and one part H_2SO_4 for 1-2 min. at room temperature, and average grain sizes measured using the linear intercept method. Densities were determined to ±0.1% by displacement in alcohol, taking the theoretical density of pure MgO single crystals as 3.584 g/cc.[11] Since pores are enlarged by chemical polishing, the average pore diameter, d, was obtained by counting the number of pores, N, in a known area, A, and using the relation[12]

$$d = 2\left(\frac{p}{\pi} \cdot \frac{A}{N}\right)^{1/2} \qquad (1)$$

where p is the volume fraction of porosity calculated from the density measurements. For Types 3, 5, and 6, this technique was only practical by omitting the clusters of extremely small pores within the grains.

Following deformation, specimens were examined with a Zeiss Linnik interference microscope (using monochromatic light having a wavelength of 0.27 μm) and with a scanning electron microscope. Thin sections of specimens of Type 1 were also examined by transmission electron microscopy, using chemical thinning techniques described elsewhere;[13] due to the residual porosity, no attempt was made to thin specimens of Types 2-6.

(3) Testing Procedure

All specimens were tested under compression in air, at temperatures in the range from room temperature to 1400°C. The specimens were placed upright in the center of a large vertical furnace with $MoSi_2$ heating elements, and held in place with alumina loading rams under a low load. The rams were protected by small alumina buttons (~0.7 in. diameter x 0.3 in. thickness) placed between the specimens and the ram surfaces, and thin (0.001 in.) Pt sheets were placed between the specimens and the buttons to act as reaction barriers. To determine strain, two sapphire rods were inserted in small holes, initially 0.5 in. apart, on one face of the specimen, and were connected externally through a lever arrangement to a linear voltage differential transformer and recorder. The testing equipment was described in detail as machine Number III by Hulse and Copley.[14]

Specimens were heated in air and held at temperature for at least 1 h prior to testing. The equipment was arranged so that all specimens were tested under a constant rate of loading of 20 psi/sec, based on the initial specimen cross-section.* Strains were continuously recorded

---

*Some investigations have directly compared tests at constant strain rate and at constant rate of loading; see, for example, Zhurkov et al.[15]

during each test to a sensitivity of $\pm 5 \times 10^{-5}$. The temperature was maintained constant to within ±2°C at temperatures of 800°C and lower, and to an estimated ±5°C at the higher temperatures.

III. RESULTS

(1) Stress-Strain Relationships

The stress-strain curves obtained for specimens of Types 1-6 are given in Fig. 2. A high slope in the curves indicates a low rate of strain and a low slope represents a high rate of strain; specimen fracture is designated by a vertical arrow. Due to machine limitations, several of the present experiments were terminated prior to fracture at total stresses of less than ∿50,000 psi.*

As shown in Fig. 2, there was a marked difference in specimen behavior at 1000°C. At this temperature, Types 1 and 2 fractured without any significant strain, Type 3 was slightly ductile, but Types 4-6 deformed to strains >0.02 prior to failure. Furthermore, Types 5 and 6 also exhibited extensive plastic strain at 800°C. All specimens were ductile at temperatures of 1200°C and above.

In general, specimens were taken to fracture to observe the overall ductility, but in a number of cases duplicate tests were terminated before fracture to permit a microstructural study during the earlier stages of plastic deformation. No significant difference in behavior was observed in these duplicate tests.

---

*Copley and Pask[1] used specimens of a slightly smaller cross-section (0.2 in. x 0.2 in.), thereby permitting total stresses of up to ∿70,000 psi on Type 6 with the same equipment.

(2) Slip Band Formation

An examination of the specimens after testing revealed several distinctive deformation characteristics. For specimens of Type 1, there was no evidence of slip in the optical microscope after tests at room temperature and 600°C, and transmission electron microscopy indicated that the grains were essentially dislocation-free. At 800°C, straight slip lines were visible in a small number of the grains, similar to those reported by Hulse et al.,[16] thus indicating that some slight plastic deformation occurred prior to fracture. Such lines arise from slip on the $\{110\}\langle 1\bar{1}0\rangle$ slip systems. Wavy slip traces occurred within the grains at temperatures of 1200°C and above, so that slip then also took place on the $\{001\}\langle 1\bar{1}0\rangle$ slip systems.

Copley and Pask[1] reported that the Type 6 specimens, in which macroscopic strain occurred at lower temperatures, exhibited wavy slip lines at 800°C. In a similar manner, wavy slip markings were visible in the two specimens of Type 5, tested at 800°C and 1000°C, respectively; and in specimens of Type 4 at 1000°C, but not at 800°C. No wavy slip lines were seen in Types 2 or 3 at tests below 1200°C. These observations are therefore consistent with the experimental data presented in Fig. 2, and indicate that slip on both the {110} and {100} planes is a prerequisite for any appreciable plastic strain.

It was also noted that, whereas the grain boundaries acted as obstacles to the low temperature planar glide, at high temperatures the wavy slip bands often extended across the boundaries and there was a tendency for bifurcation.

(3) Grain Boundary Sliding

The specimens of Type 1, being nominally fully-dense, were initially transparent.* Little or no loss in transparency was observed after testing at 800°C and below, but the specimens became translucent at 1000°C and fully opaque at testing temperatures of 1200°C and above. This loss of transparency was attributed to the occurrence of grain boundary sliding at the higher temperatures, thus leading to the formation of intergranular cavities and subsequent cracking.

Direct evidence for sliding was obtained by examining deformed specimens with an interference microscope. Although the surfaces were still relatively smooth after testing at low temperatures, the presence of sliding was clearly revealed at high temperatures by the many steps, and thus discontinuities in the interference fringes, occurring at the grain boundaries. Such steps were visible in specimens of each type, but only after testing at temperatures of 1200°C and above. It is concluded therefore that the plasticity observed in Types 5 and 6 at the lower temperatures is not significantly assisted by grain boundary sliding.

(4) Fracture Behavior

At the lower temperatures when no plastic flow took place (for example, $\leq$1000°C in Type 2), specimens of Types 2-6 failed primarily by transgranular fracture, giving many cleavage facets on the fracture surface. In specimens of Type 1, however, there was also much intergranular fracture at the lower temperatures, suggesting that the

---

*An illustration of the high degree of transparency is given elsewhere.[5]

material was weakened by the presence of residual LiF in solid solution along the grain boundaries. This difference in fracture behavior is shown by the scanning electron photomicrographs of Types 1 and 2 in Fig. 3. At the higher temperatures, fracture was almost entirely intergranular for all specimen types.

A major difference in the macroscopic fracture characteristics at low and high temperatures was also noted. At low temperatures, due to the horizontal tensile stresses, specimens tended to fracture by the vertical propagation of one or more cracks along the compressive axis;* at high temperatures, where yielding occurred, fracture took place by shear on oblique planes, resulting in fracture cones at either end of the specimen. These two fracture modes are illustrated schematically in Fig. 4.

It was also observed that specimens often contained a number of internal cracks after fracture at the higher temperatures; these appeared to be entirely intergranular in all specimens except those of Type 3. An example is shown in Fig. 5 for a Type 4 specimen tested at 1300°C. In Type 3, the cracks were occasionally of a mixed character; some transgranular cracking was evident, although to a limited extent, even at 1400°C. This is illustrated in Fig. 6 in which the crack alternates between a smooth boundary crack (A and C) and a rough transgranular crack (B). This difference in behavior may be associated with the higher impurity content of the Type 3 material, since it has been shown that SiO_2 and CaO, even though present in lesser amounts than that

---

*A similar fracture phenomenon has also been reported for fine-grained rock and glass.[17]

necessary to form a second phase, preferentially segregates at the grain boundaries when present in amounts as small as 30 atomic ppm.[18] This could impede grain boundary sliding and separation at the high temperatures, and thereby favor transgranular fracture.

Few internal cracks were observed in any specimens tested at the lower temperatures, thereby showing that, once initiated, a crack then propagates very rapidly.

IV. DISCUSSION

(1) General Characteristics of Deformation

In order to deform plastically without the nucleation of internal voids, a polycrystal must possess five independent slip systems.[19] In MgO, slip over {110} planes in $\langle 1\bar{1}0 \rangle$ directions provides only two independent slip systems, but the advent of slip over {100} planes in $\langle 1\bar{1}0 \rangle$ directions, as in wavy glide, provides a further three independent systems.[20] A complexity arises, however, since slip is not homogeneous but confined to discrete slip bands, and it is often difficult in ionic polycrystals for the various slip systems to interpenetrate; these problems are discussed in more detail elsewhere.[21]

Testing in tension, Day and Stokes[22] reported that recrystallized polycrystalline MgO was entirely brittle at temperatures below 1700°C, whilst hot-pressed material was not significantly ductile until ∿2100°C. The present results show, however, that ductility is possible in compression at temperatures as low as 800°C. This difference arises because of the greater difficulty of catastrophic failure when testing in compression, since a nucleated crack is not exposed to strong lateral tensile stresses. Larger stresses may therefore build up in compression,

and this facilitates the activation and interpenetration of the different slip systems.

It is useful to compare these polycrystalline results with those for MgO single crystals, particularly since the yield stress versus temperature relationship has been reported for the same constant rate of loading as that used in the present work.[16,23,24]

The results for single crystals having <100> and <111> loading axes are indicated by the two broken lines in Fig. 7 for temperatures in the range from -196 to 1600°C. In the former orientation, there is a resolved shear stress, equal to one half of the applied stress, acting on four of the six {110} $\langle 1\bar{1}0 \rangle$ slip systems; in the latter orientation, no resolved shear stress acts on any of the {110} $\langle 1\bar{1}0 \rangle$ slip systems and slip then takes place on the {001} $\langle 1\bar{1}0 \rangle$ systems. Since electrostatic repulsive forces inhibit the movement of dislocations of $\frac{a}{2}\langle 1\bar{1}0 \rangle$ Burgers vector on the {100} planes,[25] the yield stresses are substantially higher for the <111> orientation. The figure shows also the yield stresses obtained for the polycrystalline material: the open symbols are for specimens exhibiting some plasticity, calculated by taking a strain offset of 5×10^{-4} from the modulus line, and the closed symbol for Type 1 at 1000°C is the fracture stress when no significant yielding occurred. The yield points for Types 1-3 lie approximately on the line obtained for <111> loaded single crystals, but the points for Types 5 and 6 are somewhat lower.

Although this result at first suggests that the specimens of Types 5 and 6 yielded at the lower temperatures at stresses such that no slip was produced on the {001} $\langle 1\bar{1}0 \rangle$ slip systems, it is clear from the observations

of wavy slip that both the {110} and {100} systems were operative. Furthermore, both systems are required for polycrystalline plasticity. It appears therefore that stress concentrations can build up at the grain boundaries of these two materials of a sufficient magnitude to nucleate slip on the {100} system, and it follows that some ductility may be realized at the lower temperatures if the boundaries are sufficiently strong to support these enhanced stresses.*

(2) Effect of Differences in Material Character

The marked differences in mechanical behavior documented here are apparently due to microstructural features, in particular to variations in pore size and distribution and to the presence of impurities along the grain boundaries.

When pores are located on the boundaries, they decrease the interfacial contact area between adjacent grains, and thus weaken the material. To prevent the growth of these pores along the boundary to a critical crack length, they should therefore be few in number and small relative to the grain size. When pores are located within the grains, they impede the movement of dislocations,[27] thus giving rise to stress concentrations, but they may also allow mass accommodation by acting as dislocation sources and sinks, possibly in the manner reported for silver chloride in which dislocations were generated by the stress-field around spherical glass inclusions.[28] This suggests that mass accommodation is probably

---

*The occurrence of substantial stress concentrations at the grain boundaries was directly demonstrated in polycrystalline lithium fluoride by showing that a localized shear stress probably greater than ~9000 psi developed on a slip system on which the applied load gave a resolved shear stress of only 880 psi.[26]

aided if the intragranular pores are small in size and fairly evenly distributed.

On this basis, it is possible to interpret, at least qualitatively, the differences in behavior for the six specimen types. For Type 1, the fracture characteristics (Fig. 3) show that the grain boundaries are weak, probably due to the segregation of residual LiF which leads to easy intergranular separation. In addition, it is significant that this material exhibited the lowest fracture stresses at 800°C and 1000°C. In Type 2, low temperature ductility is inhibited by the numerous large pores on the grain boundaries, which act as crack nuclei and thus prevent the build-up of stress concentrations and consequent formation of slip on the {100} system.

Specimens of Types 5 and 6, both of which exhibit low temperature ductility, have pores on the boundaries which are small with respect to the average grain size, and clusters of very fine pores within the grains. The wide difference in grain size shows that this alone is not the important factor in promoting plasticity at the lower temperatures. It appears instead that, in the presence of relatively strong boundaries as suggested by the low impurity contents, the boundary porosity is insufficient to lead to easy intergranular cracking, and stress concentrations nucleate flow on the {001} $\langle 1\bar{1}0 \rangle$ slip systems. Some mass accommodation may also be provided by the clusters of very small pores within the grains. The possibility that pores may assist in nucleating dislocations was suggested earlier by Stokes and Li,[8] and they further postulated that nucleation may be easier when the pores are intragranular; both of these suggestions are supported by the results presented here.

It should also be noted that, whereas the Type 6 material has a fairly uniform distribution of pore clusters, Type 5 tends to have clusters only at the grain centers. This suggests that the pore clusters may be less effective in promoting ductility as the grain size is increased, particularly since the porosity is swept up during grain growth to give larger pores on the boundaries. In fact, this may account for the slightly less ductile behavior of Type 5 at 800°C and 1000°C.

For Type 3, the pore structure is similar to that of Types 5 and 6, but the Si and Ca contents are significantly higher. The lack of intergranular separation at the lower temperatures suggests that the presence of these impurities does not weaken the boundaries, in contrast to the LiF in specimens of Type 1, but rather it appears to interfere with the propagation of slip lines from one grain to the next. In addition, the pores within the grains are probably insufficient to allow substantial mass accommodation. In this respect, the character of Type 4 represents an intermediate situation between Types 3 and 6, and this is reflected by the stress-strain curves in Fig. 2.

It is concluded that the pore distribution is only of major importance in determining behavior in the temperature range where all slip band intersections are difficult, namely, at temperatures less than $\sim$1200°C when testing in compression. At temperatures of 1200°C and higher, the intersection difficulties of conjugate $\{110\}\langle 1\bar{1}0\rangle$ slip systems decrease as indicated by the development of gradual yielding and large strains at fracture in stress-strain curves obtained on single crystals with an <001> loading axis,[16,24] resulting in a decreased tendency for crack nucleation which allows the build-up of higher localized

stress levels.

V. SUMMARY AND CONCLUSIONS

Specimens of six different types of polycrystalline MgO, one nominally fully-dense and the others having various pore sizes and distributions, were tested in compression at temperatures up to 1400°C. All specimens exhibited some plastic flow prior to fracture at temperatures of 1200°C and above; but two of the materials, both ∿1% porous, also deformed plastically at temperatures as low as 800°C, and a third at 1000°C.

Plasticity at temperatures below ∿1200°C is dependent upon grain boundaries that are strong enough to allow the build up of sufficient stress concentrations to nucleate slip on the {100} system and to allow the extension of slip bands across the boundaries. A qualitative comparison of the characters of the different materials in terms of this behavior suggests the following critical factors:

(1) The boundaries should be relatively pore-free; if pores are present, they should be small with respect to the average grain size.

(2) Clusters of very fine pores within the grains appear beneficial, probably because they allow some mass accommodation by acting as sources and sinks for dislocations.

(3) The boundaries should be free from excessive amounts of impurities in solid solution since this condition may weaken them, thereby aiding intergranular separation, or may interfere with the development of slip lines within a grain and their propagation from one grain to the next.

ACKNOWLEDGMENTS

The authors are grateful to D. R. Cropper and P. E. Hart for stimulating discussions throughout the course of this work, and to N. E. Olson for experimental assistance with the mechanical testing. The scanning electron microscope was made available through Grant No. GB-6428 from the National Science Foundation and Grant No. Gm-15536 from the National Institute of Health to Professor T. E. Everhart of the Electronics Research Laboratory, University of California.

This work was supported through the Inorganic Materials Research Division of the Lawrence Radiation Laboratory by the United States Atomic Energy Commission.

REFERENCES

1. S. M. Copley and J. A. Pask, "Deformation of Polycrystalline MgO at Elevated Temperatures," J. Am. Ceram. Soc., 48 (12) 636-42 (1965).

2. S. A. Price and J. Oakley, "Notes on the Relationship between Porosity and Strength of Sintered Rings Pressed from Iron Powder," Powder Met., (12) 87-93 (1963).

3. R. W. Rice, "Production of Transparent MgO at Moderate Temperatures and Pressures," presented at the Sixty-fourth Annual Meeting, American Ceramic Society, New York, April 30, 1962 (White Wares Div. Paper No. 5-W-62); for abstract see Amer. Ceram. Soc. Bull., 41, (4) 271 (1962).

4 (a). M. W. Benecke, N. E. Olson and J. A. Pask, "Effect of LiF on Hot-Pressing of MgO," J. Am. Ceram. Soc., 50 (7) 365-68 (1967).

(b) G. D. Miles, R. A. J. Sambell, J. Rutherford and G. W. Stephenson, "Fabrication of Fully Dense Transparent Polycrystalline Magnesia," Trans. Brit. Ceram. Soc., 66 (7) 319-35 (1967).

(c) E. Carnall, Jr., "The Densification of MgO in the Presence of a Liquid Phase," Mater. Res. Bull., 2 (12) 1075-86 (1967).

(d) P. E. Hart, R. B. Atkin and J. A. Pask, "Densification Mechanisms in Hot-Pressing of Magnesia with a Fugitive Liquid," J. Am. Ceram. Soc., 53 (2) 83-86 (1970).

5. T. G. Langdon and J. A. Pask, "The Examination of Polycrystalline MgO by Transmission Electron Microscopy," in "Ceramic Microstructures" (R. M. Fulrath and J. A. Pask, eds.), John Wiley and Sons, New York, 1968, pp. 594-602.

6. W. B. Harrison, "Influence of Surface Condition on the Strength of Polycrystalline MgO," J. Am. Ceram. Soc., 47 (11) 574-79 (1964).

7. W. D. Kingery and B. Francois, "Grain Growth in Porous Compacts," J. Am. Ceram. Soc., 48 (10) 546-47 (1965).

8. R. J. Stokes and C. H. Li, "Dislocations and the Tensile Strength of Magnesium Oxide," J. Am. Ceram. Soc., 46 (9) 423-34 (1963).

9. A. G. Evans and R. W. Davidge, "The Strength and Fracture of Fully Dense Polycrystalline Magnesium Oxide," Phil. Mag., 20 (164) 373-88 (1969).

10. A. G. Evans, D. Gilling and R. W. Davidge, "The Temperature-Dependence of the Strength of Polycrystalline MgO," J. Mater. Sci., 5 (3) 187-97 (1970).

11. D. W. Budworth, "The Lattice Parameter and Density of MgO," J. Brit. Ceram. Soc., 4 (4) 481-82 (1967).

12. C. S. Smith and L. Guttman, "Measurement of Internal Boundaries in Three-Dimensional Structures by Random Sectioning," Trans. AIME, 197 (1) 81-87 (1953).

13 (a) T. G. Langdon, "Thinning of Polycrystalline MgO for Transmission Electron Microscopy," Rev. Sci. Instrum., 38 (1) 125-27 (1967).

(b) R. H. J. Hannink and T. G. Langdon, "An Electron Microscope Examination of Deformed Polycrystalline Magnesium Oxide," J. Mater. Sci., 4 (11) 1021-23 (1969).

14. C. O. Hulse and S. M. Copley, "High-Temperature Compressive Deformation Equipment," Amer. Ceram. Soc. Bull., 45 (5) 530-34 (1966).

15. S. N. Zhurkov, V. S. Kuksenko and A. I. Slutsker, "Submicrocrack Formation under Stress," in "Fracture 1969," Proc. Second Intl. Conf.

on Fracture, Brighton, England (P. L. Pratt et al., eds.), Chapman and Hall, London, 1969, pp. 531-44.

16. C. O. Hulse, S. M. Copley and J. A. Pask, "Effect of Crystal Orientation on Plastic Deformation of Magnesium Oxide," J. Am. Ceram. Soc., 46 (7) 317-23 (1963).

17. R. Seldenrath and J. Gramberg, "Stress-Strain Relations and Breakage of Rocks," in "Mechanical Properties of Non-Metallic Brittle Materials" (W. H. Walton, ed.), Butterworths, London, 1958, pp. 79-102.

18. M. H. Leipold, "Impurity Distribution in MgO," J. Am. Ceram. Soc., 49 (9) 498-502 (1966).

19. R. von Misés, "Mechanics of the Plastic Deformation of Crystals," Z. Angew. Math. Mech., 8 161-85 (1928).

20. G. W. Groves and A. Kelly, "Independent Slip Systems in Crystals," Phil. Mag., 8 (89) 877-87 (1963).

21. T. G. Langdon and J. A. Pask, "Mechanical Behavior of Single-Crystal and Polycrystalline MgO," in "High Temperature Oxides - Volume III" (A. Alper, ed.), Academic Press, New York, 1970, pp. 53-127.

22. R. B. Day and R. J. Stokes, "Mechanical Behavior of Polycrystalline Magnesium Oxide at High Temperatures," J. Am. Ceram. Soc., 49 (7) 345-54 (1966).

23. C. O. Hulse and J. A. Pask, "Mechanical Properties of Magnesia Single Crystals in Compression," J. Am. Ceram. Soc., 43 (7) 373-78 (1960).

24. S. M. Copley and J. A. Pask, "Plastic Deformation of MgO Single Crystals up to 1600°C," J. Am. Ceram. Soc., 48 (3) 139-46 (1965).

25. J. J. Gilman, "Plastic Anisotropy of LiF and Other Rocksalt-Type Crystals," Acta Met., 7 (9) 608-13 (1959).

26. W. D. Scott and J. A. Pask, "Deformation and Fracture of Polycrystalline Lithium Fluoride," J. Am. Ceram. Soc., 46 (6) 284-93 (1963).

27. A. J. Forty, "Interaction of Cavities and Dislocations in Crystals," Discs. Faraday Soc., 38 56-60 (1964).

28. D. A. Jones and J. W. Mitchell, "Observations on Helical Dislocations in Crystals of Silver Chloride," Phil. Mag., 3 (25) 1-7 (1958).

Table I. Spectrographic Analysis of Different Types of Polycrystalline MgO*

Constituent	Specimen Type, wt%						
	1	1(a)	2	3	4	5	6
Mg	Principal constituent in each type						
Si	0.003	0.003	0.007	0.1	0.03	0.02	0.015
Fe	<0.002	0.002	0.006	0.003	0.004	<0.002	-
Al	0.001	0.001	0.007	0.001	0.002	0.001	<0.005
Cu	0.0005	0.0005	<0.0005	<0.0005	0.0007	<0.0005	0.0008
Li	0.0075	0.15	-	-	-	-	-
Ni	<0.001	<0.001	-	-	-	-	-
Sr	<0.005	<0.005	<0.005	<0.005	<0.005	<0.005	<0.005
Cr	-	-	0.0008	-	<0.0008	<0.0008	-
Ba	-	-	-	<0.002	-	-	-
Ca	0.004	0.005	0.01	0.08	0.02	0.008	0.02
	0.0165†	0.0175†	0.0363	0.1915	0.0625	0.0373	0.0458

*Constituents reported as oxides of the elements indicated, with the exception of Li in Types 1 and 1(a) which was probably present as LiF. Analysis performed by American Spectrographic Laboratories, Inc., San Francisco, California.

† Li not included in total.

Table II. Primary Characteristics of the Different Specimen Types

Specimen Type	Average grain size (μm)	Average density (g/cc)	Density as a %	Average pore dia. (μm)	Ratio of pore size on boundary to grain size
1	12	3.577	>99.8%	(No pores visible)	
2	20	3.528	>98.4%	2.5*	0.20
3	40	3.535	>98.6%	2.0	0.05
4	45	3.515	>98.0%	1.0	0.02
5	80	3.536	>98.6%	4.0	0.05
6	25	3.546	>98.9%	1.0	0.04

*Average size of pores on boundary alone $\sim$4 μm.

FIGURE CAPTIONS

Fig. 1. Microstructures of each specimen type.

Fig. 2. Stress-strain curves for each specimen type tested at a constant rate of loading of 20 psi/sec.

Fig. 3. Scanning electron photomicrographs of the fracture surfaces of specimens of Types 1 and 2 tested at room temperature.

Fig. 4. Mode of fracture at (a) low temperatures, (b) high temperatures.

Fig. 5. Intergranular crack in specimen of Type 4 tested at 1300°C.

Fig. 6. Mixed intergranular (A and C) and transgranular (B) crack in specimen of Type 3 tested at 1400°C.

Fig. 7. Yield stress versus temperature for the {110} $\langle 1\bar{1}0 \rangle$ and {001} $\langle 1\bar{1}0 \rangle$ slip systems, corresponding to single crystals with <100> and <111> stress axes, and the yield (open symbols) and fracture (closed symbol) stresses for polycrystalline specimens of Types 1-6.

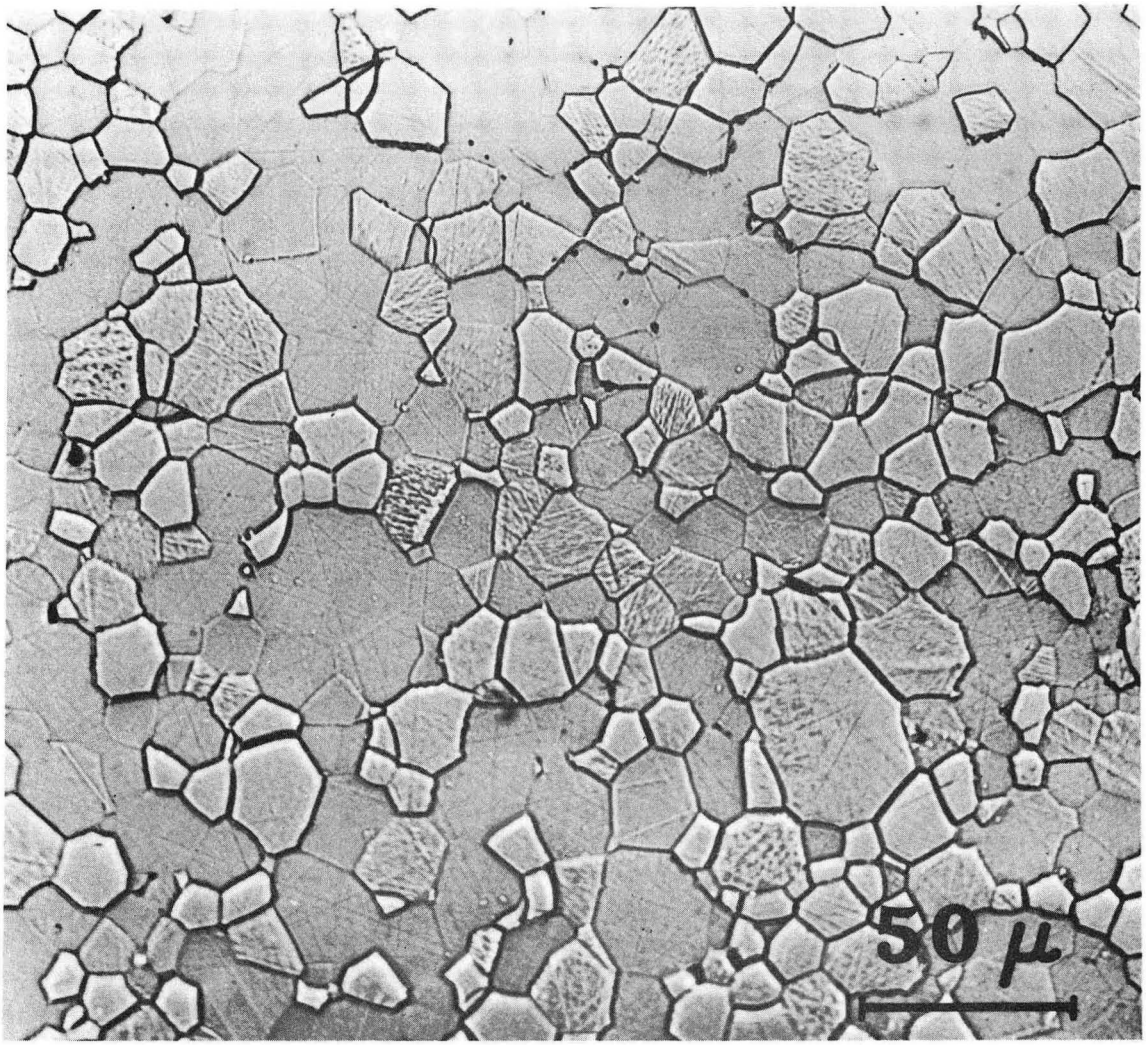

XBB679-5516

Fig. 1-1.

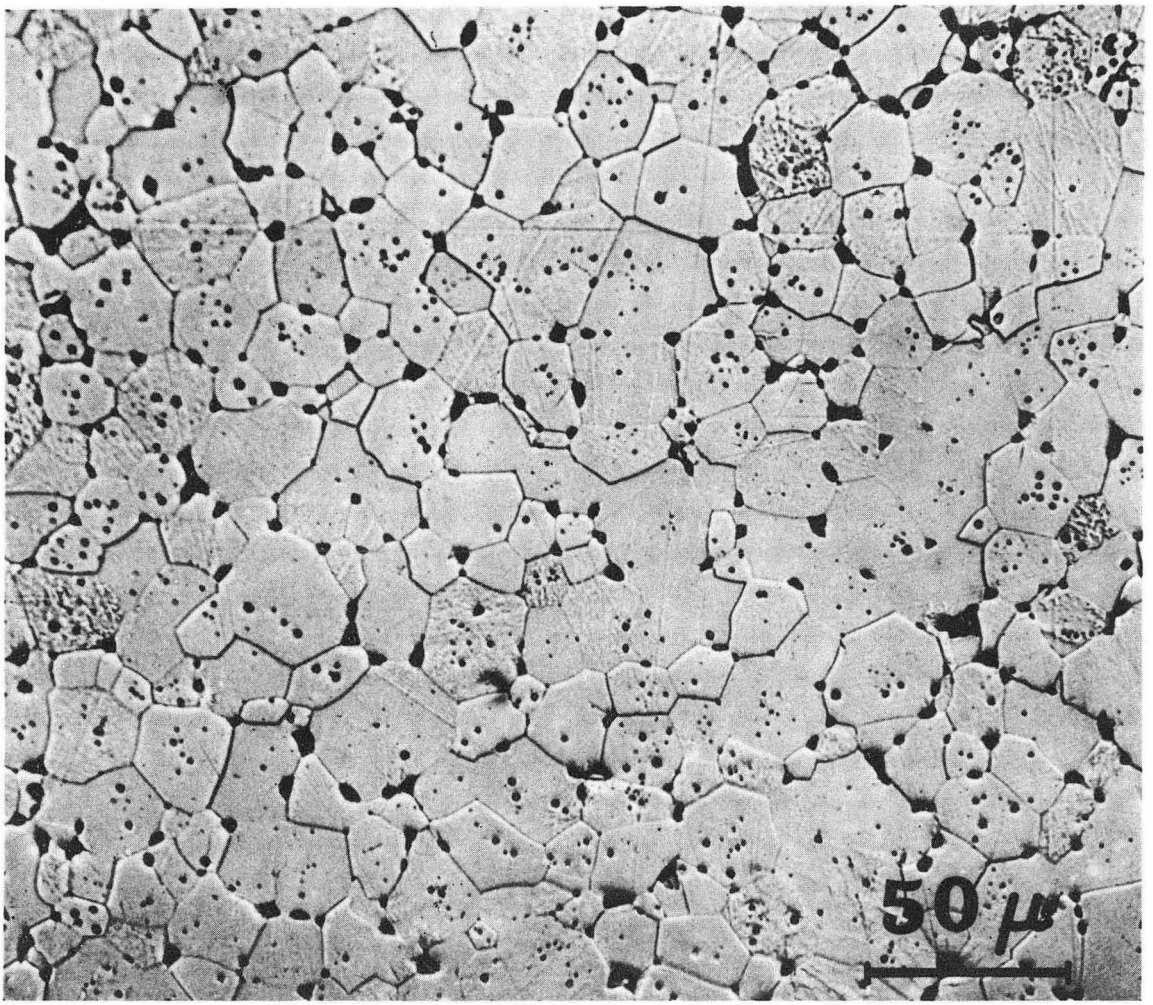

XBB679-5520

Fig. 1-2.

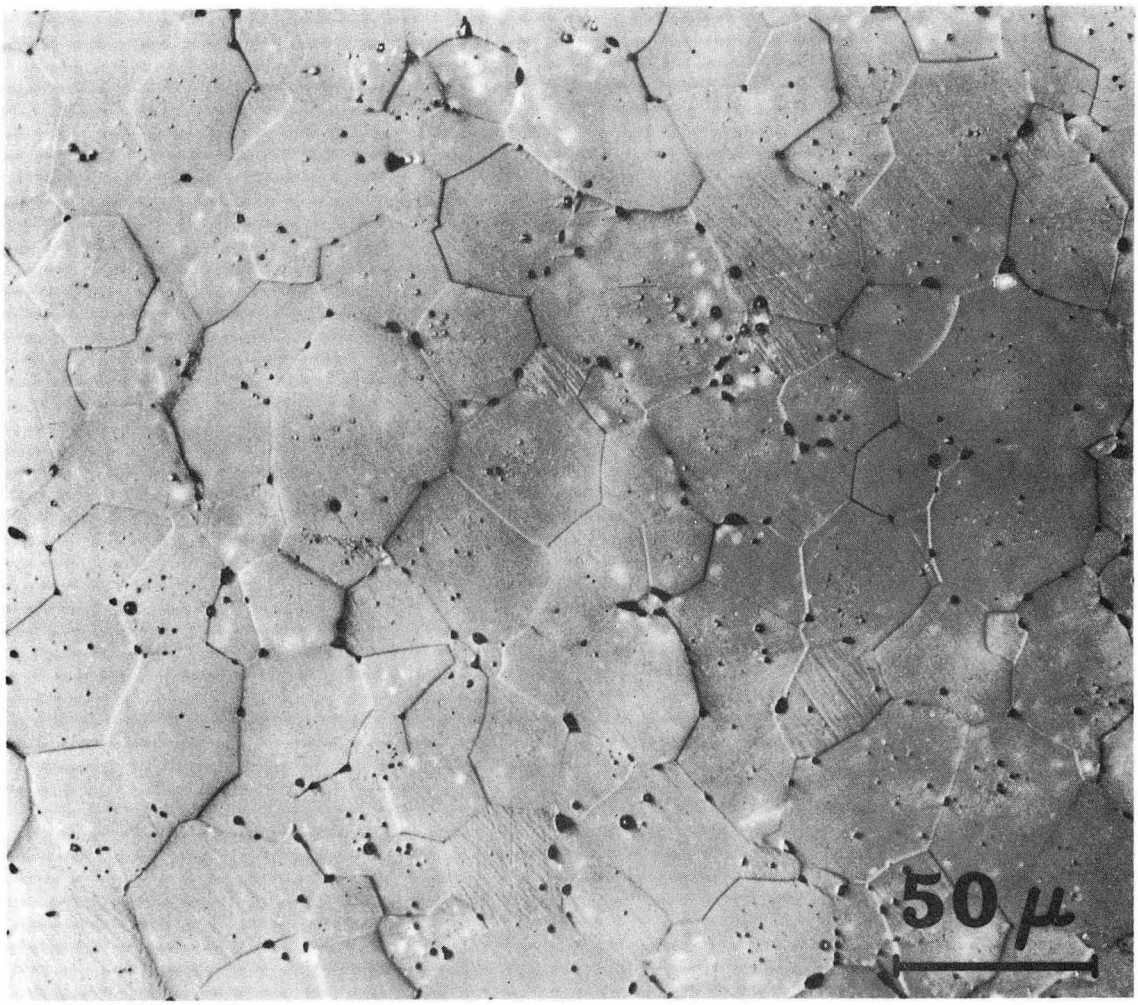

XBB679-5517

Fig. 1-3.

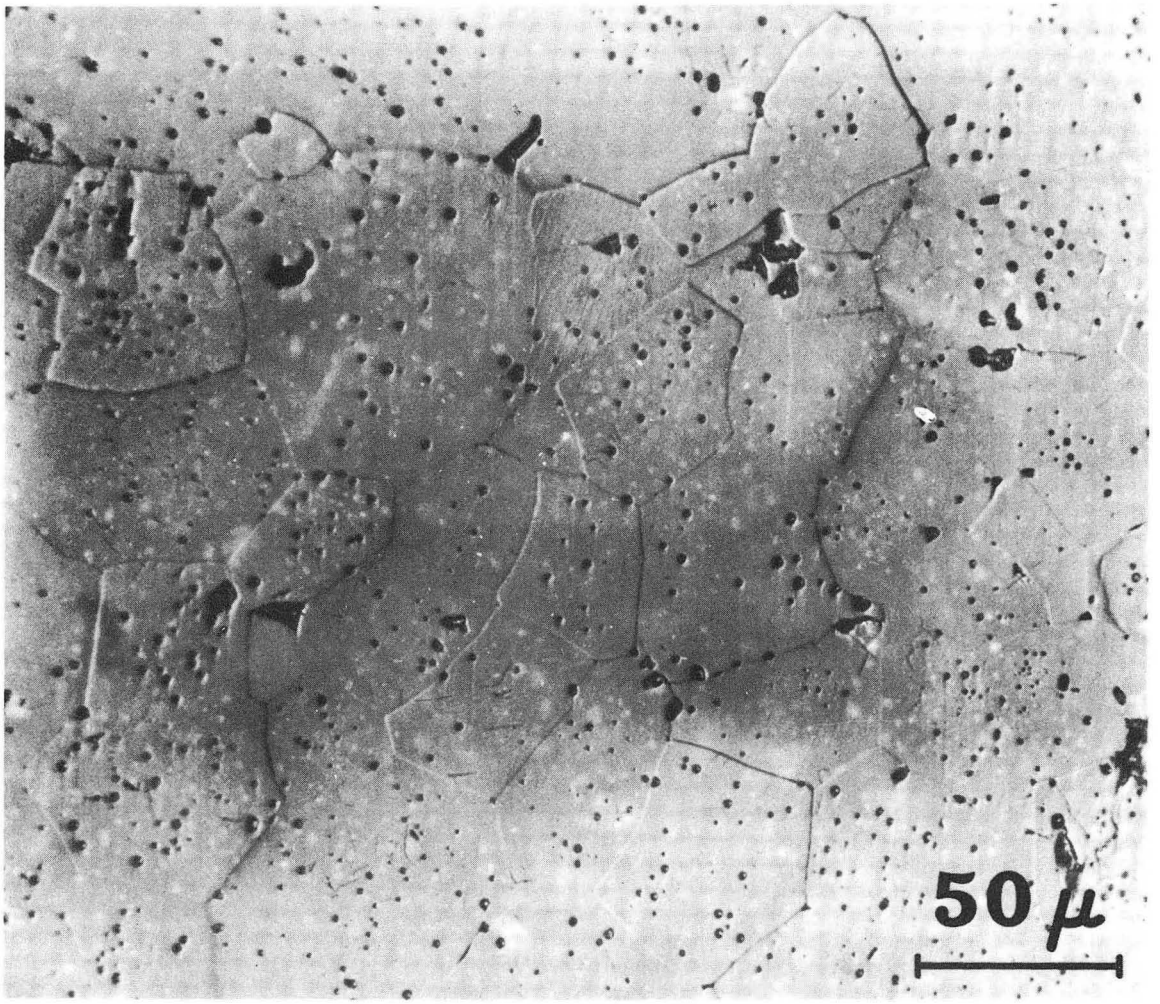

XBB679-5518

Fig. 1-4.

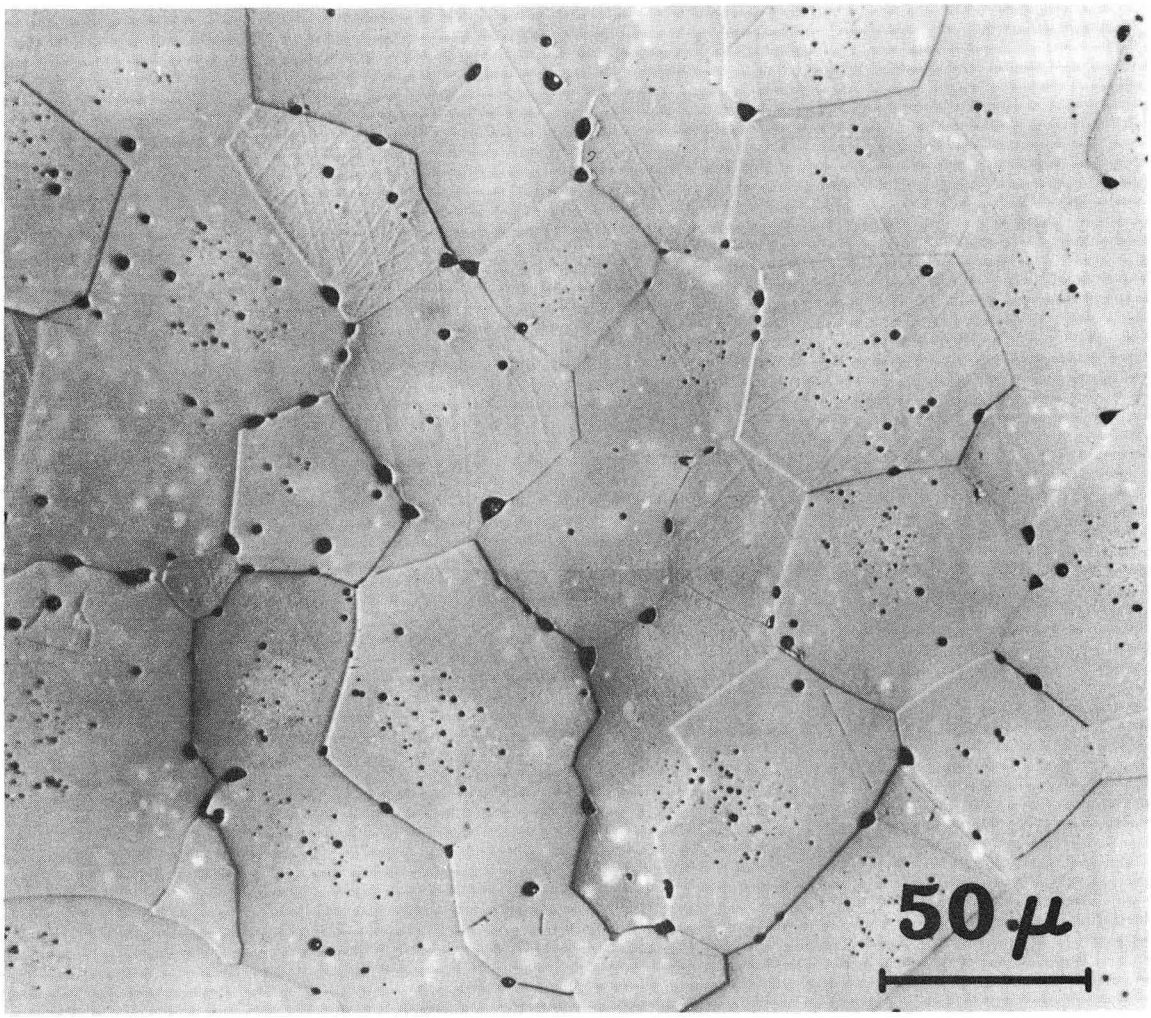

XBB679-5519

Fig. 1-5.

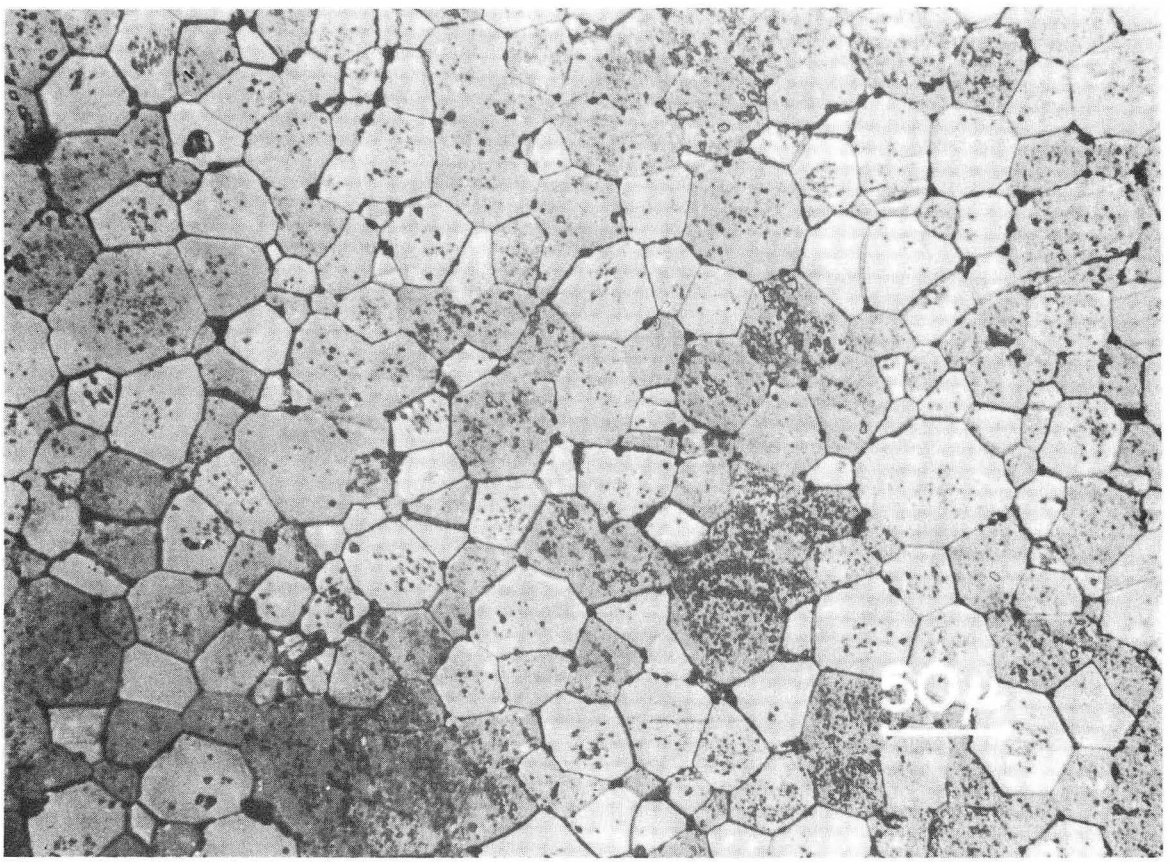

IM-1253

Fig. 1-6.

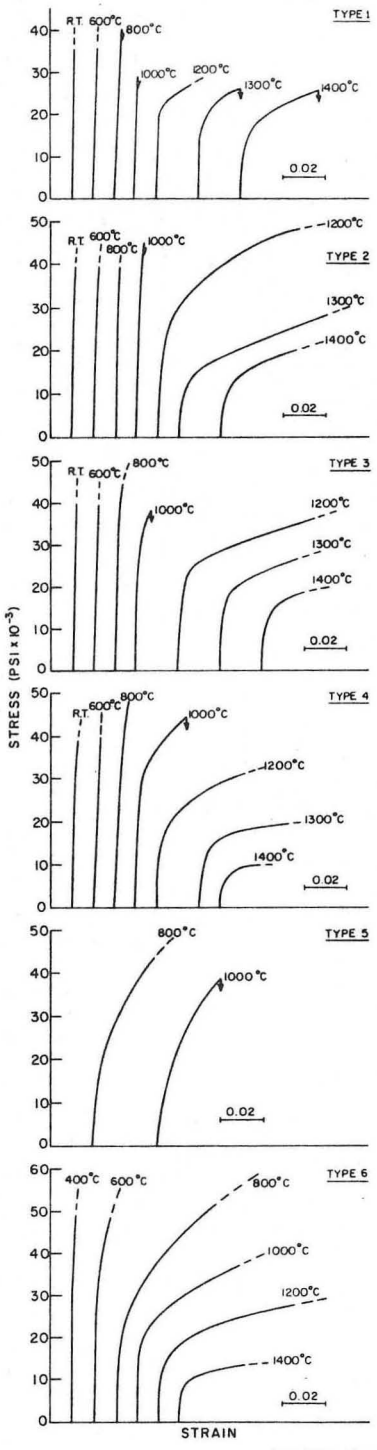
TYPE 1
R.T
600°C
800°C
1000°C
1200°C
1300°C
1400°C
0.02
TYPE 2
R.T
600°C
800°C
1000°C
1200°C
1300°C
1400°C
0.02
TYPE 3
R.T
600°C
800°C
1000°C
1200°C
1300°C
1400°C
0.02
TYPE 4
R.T
600°C
800°C
1000°C
1200°C
1300°C
1400°C
0.02
TYPE 5
800°C
1000°C
0.02
TYPE 6
400°C
600°C
800°C
1000°C
1200°C
1400°C
0.02
STRESS (PSI x 10⁻³)
STRAIN
XBL 7010-6718

Fig. 2.

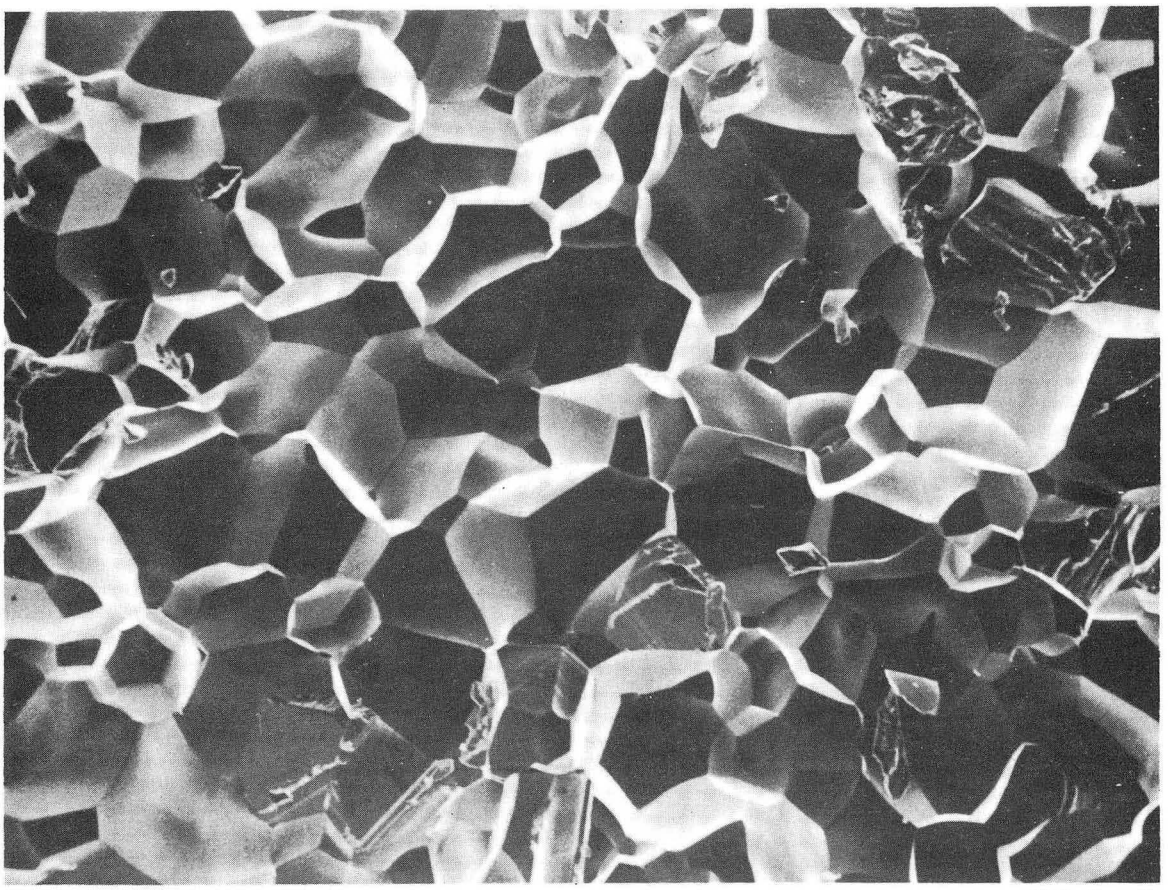

XBB688-4706

Fig. 3-1.

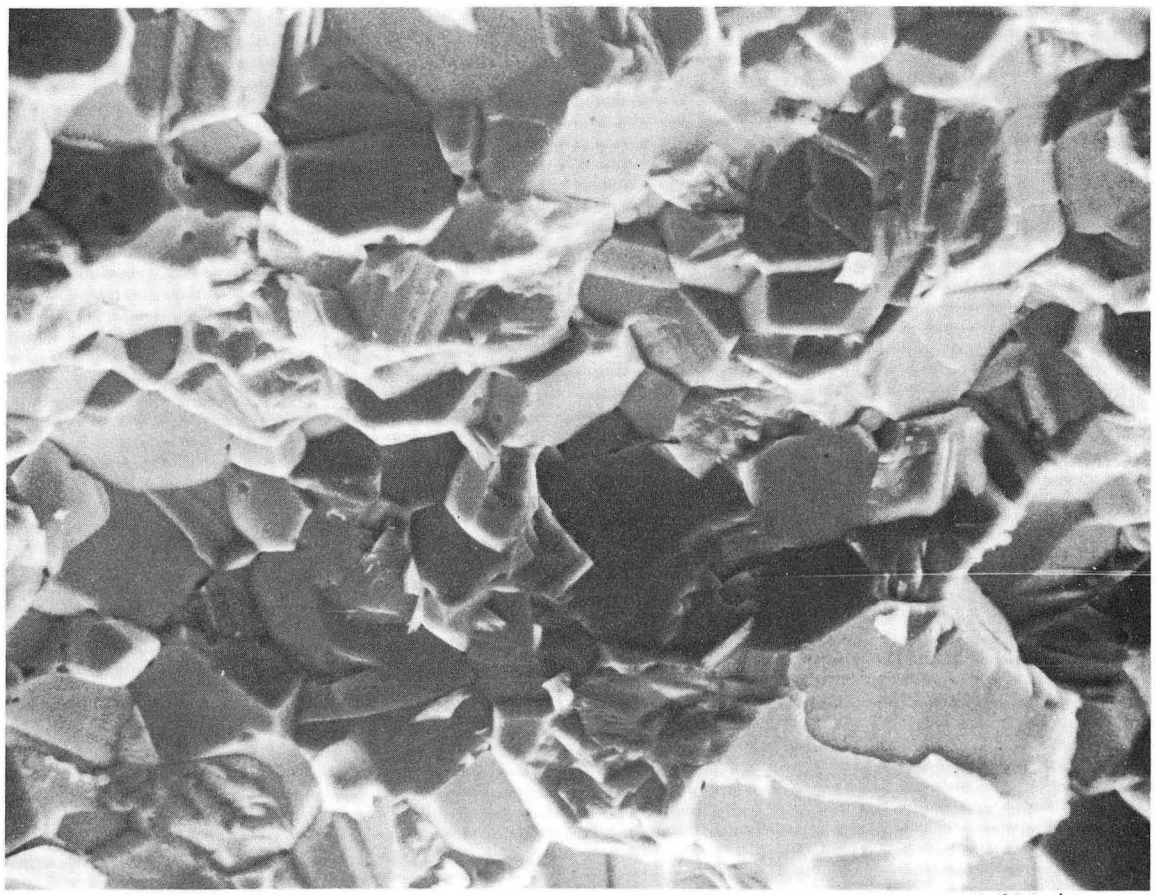

XBB688-4710

Fig. 3-2.

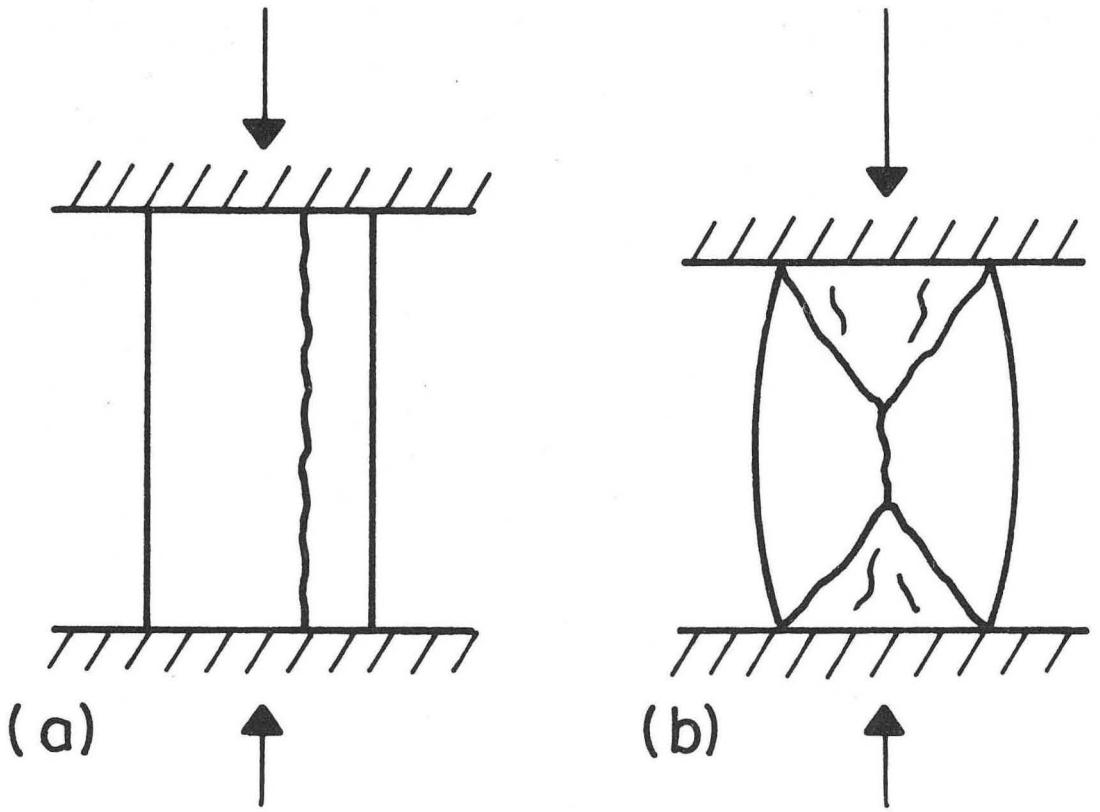

XBL 7010-6720

Fig. 4.

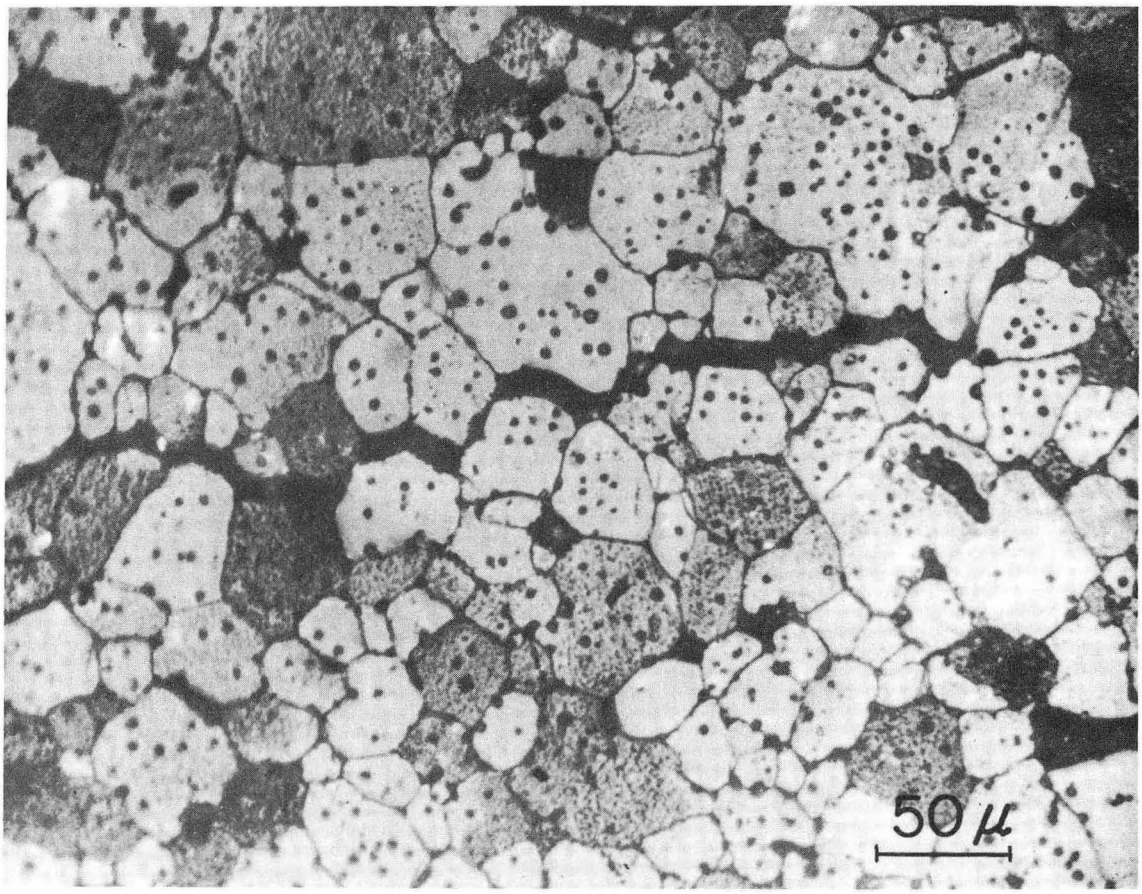

XBB7011-5305

Fig. 5.

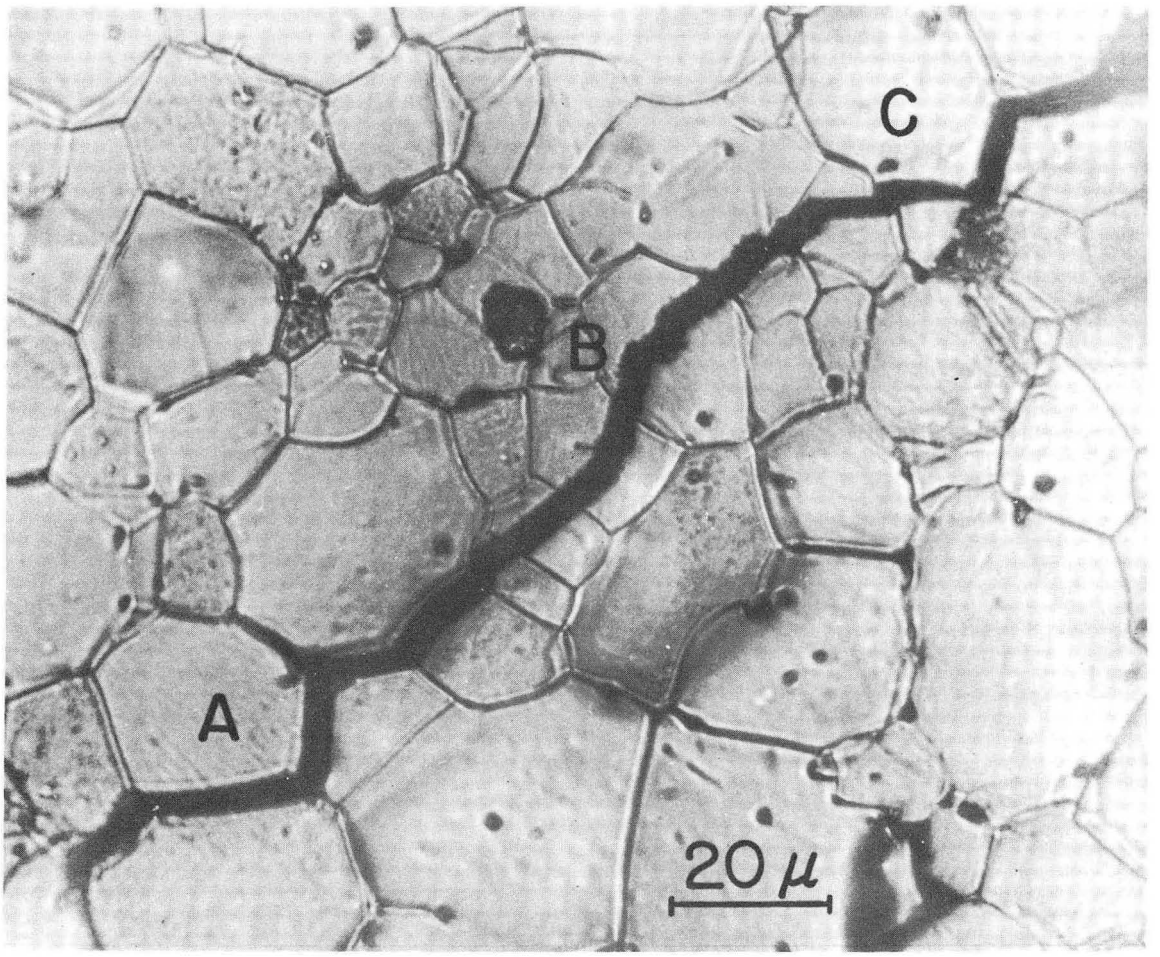

XBB7011-5306

Fig. 6.

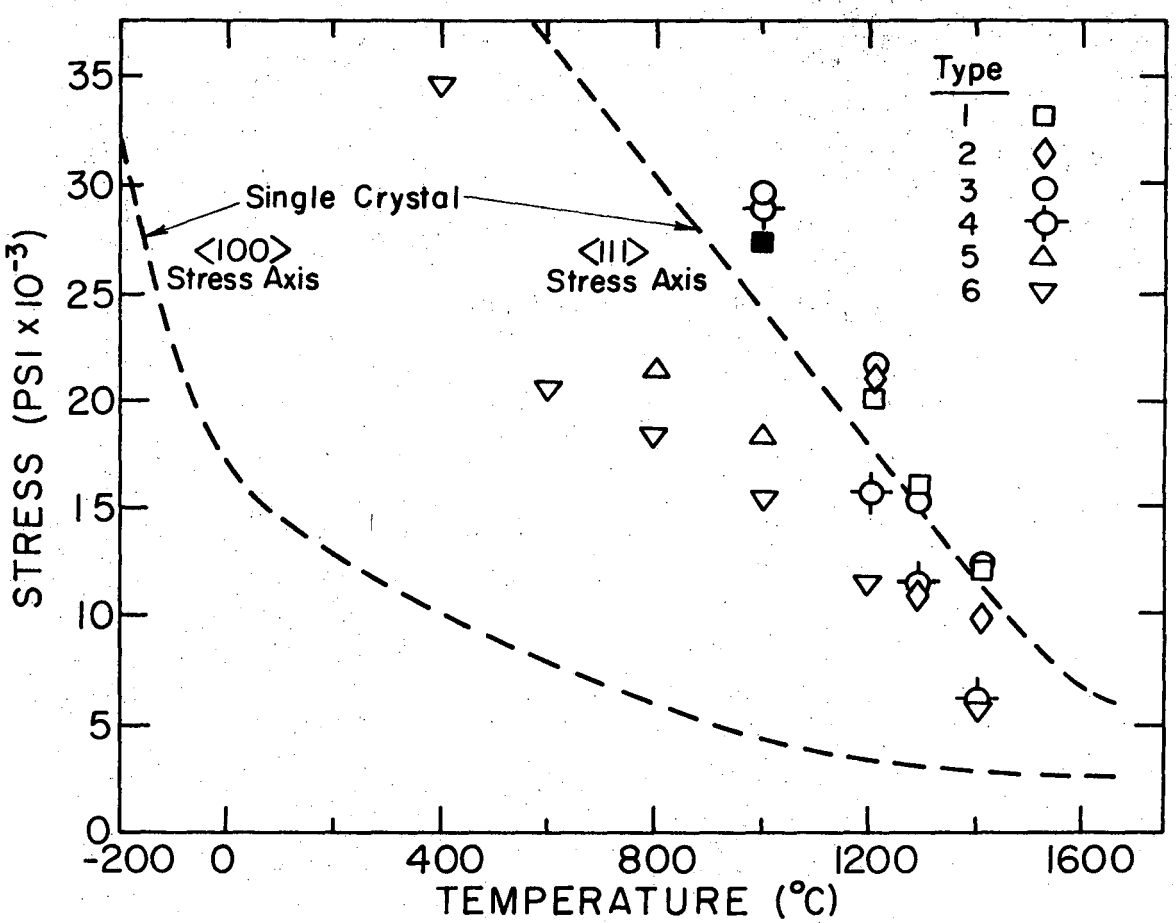

XBL 7010-6721

Fig. 7.

LEGAL NOTICE

TECHNICAL INFORMATION DIVISION
LAWRENCE RADIATION LABORATORY
UNIVERSITY OF CALIFORNIA
BERKELEY, CALIFORNIA 94720